Adsorption 2, 77–87 (1996)

Diffusion of Short-Chain Molecules on Metal Surfaces

KRISTEN A. FICHTHORN
Departments of Chemical Engineering and Physics, The Pennsylvania State University, University Park, PA 16802

Abstract. In this paper, we review our recent theoretical and simulation studies of the surface diffusion of *n*-alkanes, ranging in size from ethane to hexadecane, physically adsorbed on Pt(111). The model system exhibits many features seen experimentally. Through both animation of the molecular trajectories and determination of the minimum-energy path for nearest-neighbor hopping, we find that the shorter molecules (ethane through octane) all have similar diffusion mechanisms, involving coupled translation and rigid rod-like rotation in the surface plane. In addition, the diffusion energy barriers for these molecules increase nearly linearly with chain length in both the static and dynamic calculations. The diffusion of decane and hexadecane does not adhere to the trends for the shorter molecules and a decrease can be observed in the dynamical diffusion energies for these molecules. The diffusion of the longer molecules involves hops, with unique mechanisms, to second and third neighbor sites. Our static analysis has indicated, for decane, that the diffusion-energy barrier for third-neighbor hopping is lower than that for nearest-neighbor hopping and is in agreement with the trend seen in the dynamical diffusion barriers. Even though there is agreement between theoretical and simulated diffusion energy barriers for many of the molecules, the motion observed in the MD simulations does not agree with the assumptions of the hopping model. A model that can incorporate the influence of long flights would provide a more realistic description of the motion.

Keywords: diffusion, molecular-dynamics simulation

Introduction

Since the 1920's, when studies of crystal growth sparked interest in transport over surfaces, the diffusion of adsorbed species on solid surfaces has been a topic of considerable study. Surface diffusion is a fundamental rate process underlying several areas of technological interest. For example, the progress of catalytic-surface reactions is influenced by the mobility of adspecies. Surface diffusion can be crucial to separations involving membranes or zeolites. In addition, the mobility of adsorbed species can be critical in determining the structure and properties of thin films. Hence, the role of surface diffusion in technologies involving coating, adhesion, tribology, and deposition is also significant.

Despite its prominence in many interfacial phenomena, the knowledge of surface diffusion has been limited primarily to the study of atoms. In recent years, a few experimental studies (Arena et al., 1990; Brand et al., 1990; Reutt-Robey et al., 1988; Stranick et al., 1994) have begun to probe the diffusion dynamics of adsorbed molecules. Unlike atoms, molecules have rotational and internal degrees of freedom, creating the possibility for complex and interesting diffusion mechanisms, even in the most simple molecular adsorbates (Wang and Fichthorn, 1993; 1995). At this stage, most measurements are "macroscopic" and do not contain sufficient detail to resolve microscopic details of diffusion. However, with recent advances in experimental techniques, such as scanning-tunneling microscopy (STM), it has become possible to resolve some features of the internal structure of an adsorbed molecule (Hallmark et al., 1993) and to follow dynamical details of surface diffusion in ultra-high vacuum studies on well-defined, single-crystal surfaces (Ganz et al., 1992; Stranick et al., 1994). Hence, the capability to experimentally determine microscopic features of surface diffusion is rapidly emerging. The possibility of revealing new and interesting diffusion mechanisms is intriguing from a scientific point of view. In addition, such capabilities have important ramifications for the

development of rigorous and accurate theory, which can find application in design.

Molecular-level simulation and analysis can provide important insight to experimental results, since details of molecular diffusion that are difficult to probe experimentally can be thoroughly studied with these techniques. Molecular-dynamics (MD) simulations have proven to be a powerful technique for resolving microscopic details of diffusion at high temperatures relative to the diffusion barrier (Cohen and Voter, 1989). As the temperature decreases, adsorption becomes increasingly localized to a set of binding sites and the time between successive "hops" of an adsorbate between binding sites increases. MD simulations are not practical at low temperatures because they cannot probe the long-time scale for intersite motion. Since the dynamics of infrequent events is closely related to the adsorbate-surface potential-energy-surface (PES) topology, another useful approach for studying surface diffusion is to construct maps of the PES (Wang and Fichthorn, 1993; 1995). From these maps, adsorption sites molecular conformations, minimum-energy paths for motion between neighboring binding sites, diffusion-energy barriers, and detailed mechanisms can be obtained. Transition-state theory (TST) provides a theoretical framework for constructing surface-diffusion coefficients from this information. It is also possible to obtain diffusion coefficients from MD simulations and estimates from both techniques (MD and TST) can be used to interpret experimental values with added molecular-level insight.

In addition to aiding in the interpretation of experimental results, MD and TST provide a test of theories for describing diffusion dynamics. In analysis of experimental data, it is often assumed that surface diffusion adheres to a nearest-neighbor hopping model, in which TST provides the diffusion coefficient. However, in recent experimental studies, Arrhenius parameters have been reported that seem unreasonable physically (Brand et al., 1990). These and other experimental observations (Arena et al., 1990; Ganz et al., 1992) have raised doubts regarding the general applicability of the hopping model. By comparing diffusion coefficients obtained in MD simulations to those calculated using TST, we can assess the accuracy of the hopping model and identify features that should be included in a more rigorous theory.

In this paper, we review our recent theoretical and simulation studies (Fichthorn et al., 1994; Huang et al., 1994a, b) of the diffusion of n-alkanes physically adsorbed on a Pt(111) surface. Our work has been partly motivated by the experimental studies of Brand et al. (1990) who used laser-induced thermal desorption (LITD) to investigate the diffusion dynamics of short n-alkanes (propane through n-hexane) that physically adsorb on Ru(001). For this series, they observed that both the diffusion and desorption energies scale linearly with chain length. They conjectured that the linear trends resulted from the similarity of the binding conformations and the diffusion mechanisms for the series. These studies also discussed several interesting features that may be associated with n-alkane diffusion, including multiple-binding conformations and novel dynamical behavior. By probing the dynamics in our model system, using MD, and exploring characteristic diffusion mechanisms, using TST, we can gain insight into the results of the experimental studies. In addition, our studies can indicate the most fruitful direction for theoretical analysis. Below, we discuss our models, methods, and the insight that these studies have provided.

Model

Our model system is comprised of surface atoms and a single n-alkane adsorbate. In modelling the Pt(111) surface, a five-layer slab, which contained 36 to 64 atoms per layer, was utilized. The Pt-Pt interaction was modeled using a Lennard-Jones (6–12) potential (Halicioglu et al., 1975) and a cut-off radius of $2.5\sigma_s$, where σ_s is the Lennard-Jones length parameter. The Lennard-Jones potential provides computational economy and has been found to represent the surface phonon spectrum of fcc(111) metals with good accuracy (Allen et al., 1971). Atoms in the top three layers followed Newton's equation of motion. The equations of motion were integrated using the Verlet algorithm with a time step of 2 fs. The fourth-layer atoms were maintained isothermal by means of the Gaussian thermostat method (Nosé, 1991; Hoover et al., 1982; Evans, 1983). The equations of motion for these atoms are given by

$$\dot{\boldsymbol{p}}_i = -\nabla_{r_i} U - \zeta \boldsymbol{p}_i, \tag{1}$$

where $\boldsymbol{p}_i$ is the momentum of atom i, U is the potential energy, and ζ is a quantity akin to a friction coefficient that is adjusted at each time step to constrain the instantaneous kinetic temperature to a desired value. The integration scheme for atoms in the fourth layer and the determination of ζ for each time step was done

via a method proposed by Brown and Clarke (1984). Atoms in the fifth layer were fixed to the equilibrium platinum crystal-lattice positions to provide a structural template for the atoms above. Periodic boundary conditions were applied in the x and y directions parallel to the surface.

The n-alkanes were modeled with the united-atom (UA) model, developed by Ryckaert et al. (Ryckaert and Bellemans (1978), Catlow et al. (1990)), in which methyl and methylene groups are represented by a single interaction center and distinguished only by mass. In the UA model, the internal degrees of freedom include C—C stretching, C—C—C bond-angle bending, and torsion about nonterminal C—C bonds. The high-frequency C—C stretch was neglected by constraining the carbon-carbon bond length to its fluid-phase equilibrium value. By constraining the C—C stretch, we alter the Hamiltonian and the system is not equivalent to one in which the C—C bonds are modeled by a harmonic potential—even in the limit of very strong force constants (Fixman, 1974). Correction terms are necessary if the bond-angles depart significantly from their equilibrium values. However, since the degree of bond-angle bending is not significant in our study (see below), we have ignored these corrections. Our model for the internal degrees of freedom includes the bond-angle bending and torsional modes, which were modeled by appropriate potential-energy functions (Ryckaert and Bellemans, 1978; van der Ploeg and Berendsen, 1986). A direct Lennard-Jones (6–12) interaction (Ryckaert and Bellemans, 1978), between a united-atom i and united-atom j in the alkane molecule for $j > i + 3$, was also included. The intramolecular Lennard-Jones interaction between united atoms prevents distant united-atom segments from becoming unphysically close to one another. The alkane-Pt interaction was modeled by a Lennard-Jones (6–12) potential. The value of the length parameter for the alkane-Pt interaction σ_{ms} was obtained using the Lorentz-Berthelot mixing rule (Allen and Tildesley, 1987), which gives $\sigma_{ms} = 3.231$ Å, from the average of the Lennard-Jones σ parameters for the Pt-Pt interaction and the fluid-phase interaction between united atoms (Ryckaert and Bellemans, 1978). The value of $\varepsilon_{ms}/R(= 156.35\ \text{K})$ was chosen to approximately match the experimental heat of adsorption for n-butane on Pt(111) (Salmeron and Somorjai, 1981).

The Lagrange equation of motion for molecules with intramolecular constraints (Ryckaert and Bellemans, 1978) was used to model the motion and is given, for united atom i with mass m_i, by

$$m_i\ddot{\boldsymbol{r}}_i = -\nabla_{r_i} U - \sum_{k=1}^{l} \lambda_k \frac{\partial \sigma_k}{\partial \boldsymbol{r}_i}. \tag{2}$$

Here, $\{\lambda_k\}(k = 1, l)$ is a set of Lagrange multipliers requiring that the solution of Eq. (2) satisfy the constraints of fixed C—C bond lengths to the equilibrium distance of d_{CC}. The constraints $\{\sigma_k\}$ are given by

$$\sigma_k = (\boldsymbol{r}_{i+1} - \boldsymbol{r}_i)^2 - d_{CC}^2 = 0. \tag{3}$$

The equations of motion were integrated using the Verlet algorithm in conjunction with the SHAKE algorithm of Ryckaert et al. (1977), to maintain fixed C—C bond lengths.

To study the dynamics of surface diffusion, MD simulations were run for each n-alkane (ethane through hexadecane) species for at least five temperatures in the range of 15–350 K. For each temperature, twenty simulations, each with a length of 500 ps, were run to obtain trajectory data. Each run consisted of an equilibrium phase, in which the velocities of all particles were adjusted to achieve the desired temperature, followed by a simulation run. In all of the results reported here, the average temperature of the molecule was within one percent of the desired temperature.

To obtain characteristic mechanisms of n-alkane motion, we determined the minimum-energy paths for motion between neighboring binding sites. The binding sites were identified through a search in which a unit cell of the fcc Pt(111) surface was partitioned into a grid. Fixing the alkane center of mass at each (x, y) grid point, we used Metropolis Monte Carlo simulated annealing to vary the remaining degrees of freedom to minimize the potential energy at that grid point. The minimum-energy location and conformation were selected as the binding site and the binding conformation, respectively. In MD simulations run at the lowest temperatures, adsorption was found to be localized at these locations and conformations.

In the case of ethane, the minimum-energy pathway for motion between neighboring binding sites could be obtained from the map of minimum energy vs. the x and y center-of-mass coordinates of the molecule that was created in the search for the binding site. Figure 1 shows this plot and indicates the locations of the potential-energy minima and saddle points. By sequencing molecular conformations along the approximate pathway of steepest ascent from the binding site to the transition state, a continuous pathway

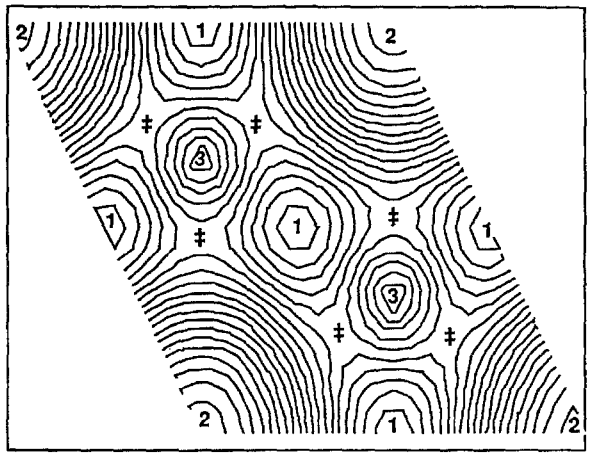

Figure 1. Contour map of the minimum potential energy of ethane for various center-of-mass locations over a unit cell on the Pt(111) surface. Positions marked 1 are global minima, at bridge sites between two Pt atoms. Positions marked 2 are global maxima, directly above Pt atoms. Positions marked 3 are local maxima, above three-fold sites. Positions marked ‡ are saddle points.

of conformations could be formed. However, for the longer alkanes, the map produced a discontinuous pathway and more sophisticated methods were required to obtain the correct diffusion mechanisms and activation barriers. For the longer molecules, we used a variant of the Elastic-Band method developed by Mills and Jónsson (1995) for use in their studies of dissociative adsorption (Mills and Jónsson, 1994) and the diffusion of metal atoms on metal surfaces. In this method, two images of the molecule are fixed at the minimum-energy conformations at neighboring binding sites. A pathway is formed by distributing a set of images between the two images fixed at each binding site. Neighboring images along the pathway are connected by Hookean springs. To converge to the minimum-energy path for $P+1$ images, an object function is defined as

$$U(\boldsymbol{R}_1, \boldsymbol{R}_2, \ldots, \boldsymbol{R}_{P-1}) = \sum_{i=1}^{P-1} U(\boldsymbol{R}_i) + U^S, \qquad (4)$$

where $\boldsymbol{R}_1, \boldsymbol{R}_2, \ldots, \boldsymbol{R}_{P-1}$ are the configurations of the $P-1$ images between the two binding sites, $U(\boldsymbol{R}_i)$ is the potential energy of image i, including both intramolecular and molecule-surface interactions, and U^S is the spring energy, which is of the form

$$U^S = \sum_{i=1}^{P+1} \frac{kP}{2} (\boldsymbol{R}_i - \boldsymbol{R}_{i-1})^2. \qquad (5)$$

In Eq. (5), k is the spring constant. The Metropolis Monte Carlo method was used to minimize the object function via simulated annealing. The set of images resulting from the minimization provides an estimate of the diffusion pathway. The diffusion barrier is given by the energy difference between the maximum energy along the pathway and the minimum energy of the image at the binding site.

Two variables in this method are P and the spring constant k. If the spring constant is too small, the minimization will result in all images residing in the two minima, with a diffusion barrier of zero. As the spring constant is increased, images begin to distribute along the pathway. With too few images, it is possible to underestimate the diffusion barrier, because the images will be sparsely distributed and it becomes unlikely that an image will be located at the maximum along the pathway. Figure 2 shows the influence of P and k on the value of the diffusion barrier for n-octane. It can be seen that the diffusion barrier increases as both P and k increase. For $P \geq 100$ and $k \geq 200$, the barrier has converged to a value of 5.2 kJ/mol.

Similarly to recent methods that have been developed for identifying reaction coordinates (Sevick et al., 1993; Ionova and Carter, 1994), the Elastic-Band method does not require *a priori* knowledge of the first-order saddle point, which is the maximum along the minimum-energy pathway connecting neighboring minima. At both the minimum and the saddle point, the gradient in potential energy is zero. Moreover, the Hessian matrix, consisting of the second derivatives of the potential energy with respect to all degrees of freedom, has all positive eigenvalues at the minimum and just one negative eigenvalue (with the rest positive) at the saddle point. In order to confirm the ability of the simulated annealing method to converge to minima and the ability of the Elastic-Band method to yield saddle points, we calculated the gradient of the energy and the Hessian matrix at all critical points. Details of these calculations will be discussed elsewhere (Chen and Fichthorn, 1995). The energy derivatives were obtained in terms of generalized coordinates (i.e., bond angles, torsion angles, etc.) as opposed to Cartesian coordinates. In all cases discussed below, the eigenvalues of the Hessian confirmed the identities of the critical points. In addition, our observation of the low-temperature MD trajectories further confirmed the feasibility of the mechanisms elucidated by the minimum-energy pathways.

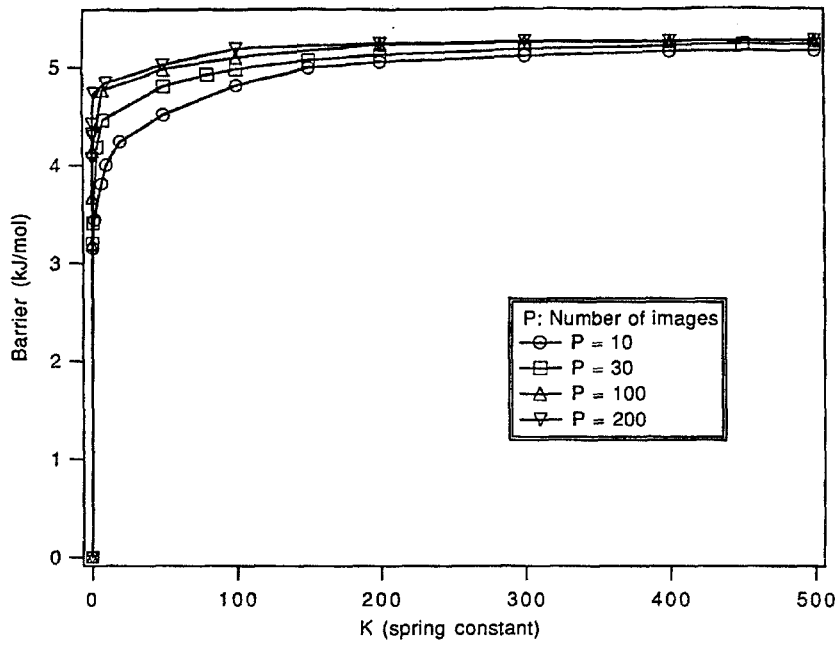

Figure 2. Plot of diffusion-energy barrier for octane from the Elastic-Band method as a function of spring stiffness for 10, 30, 100, and 200 images.

Results and Discussion

Two "macroscopic" quantities that characterize adsorption and diffusion dynamics are the desorption energy and the tracer-diffusion coefficient, respectively. These quantities can be obtained from the MD simulations. We determined the tracer-diffusion coefficient D using the Einstein equation for two-dimensional motion, given by

$$\langle l^2 \rangle = 4Dt \tag{6}$$

Here, $\langle l^2 \rangle$ is the mean-square displacement and t is time. We measured the mean-square displacement as an ensemble average over varying time intervals. Figure 3 shows a plot of $\langle l^2 \rangle$ vs. t for decane at 250 K. It can be seen that the plot is linear in the long-time limit. We obtained the diffusion coefficient from the slope of a plot of $\langle l^2 \rangle$ vs. t at long times. From Arrhenius plots of the tracer-diffusion coefficients as a function of temperature (Huang et al., 1994a), we obtained the values of the activation energy E_d and the preexponential factor D_0 for each of the n-alkanes studied. These values are plotted against chain length in Fig. 4.

As a measure of the desorption activation energy E_{des}, we calculated the time-averaged potential energy

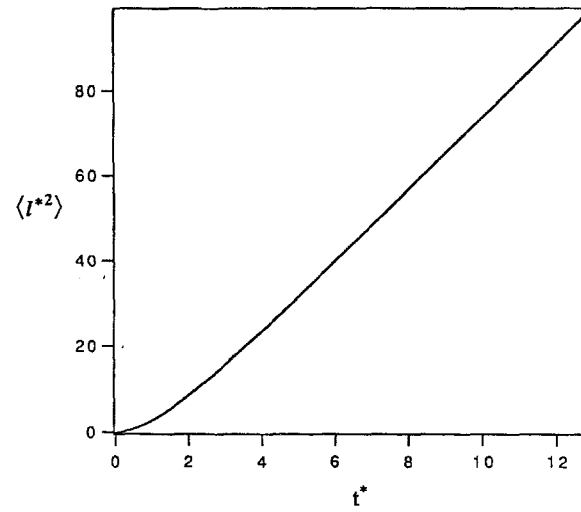

Figure 3. Dimensionless mean-square displacement as a function of dimensionless time for decane at 250 K.

of an adsorbed molecule at an intermediate temperature in the range probed. The potential energy is dominated by the molecule-surface interaction—the intramolecular energy of the adsorbed molecule and the intramolecular energy of the molecule in the gas phase, the latter of which we took to be zero, are small in comparison.

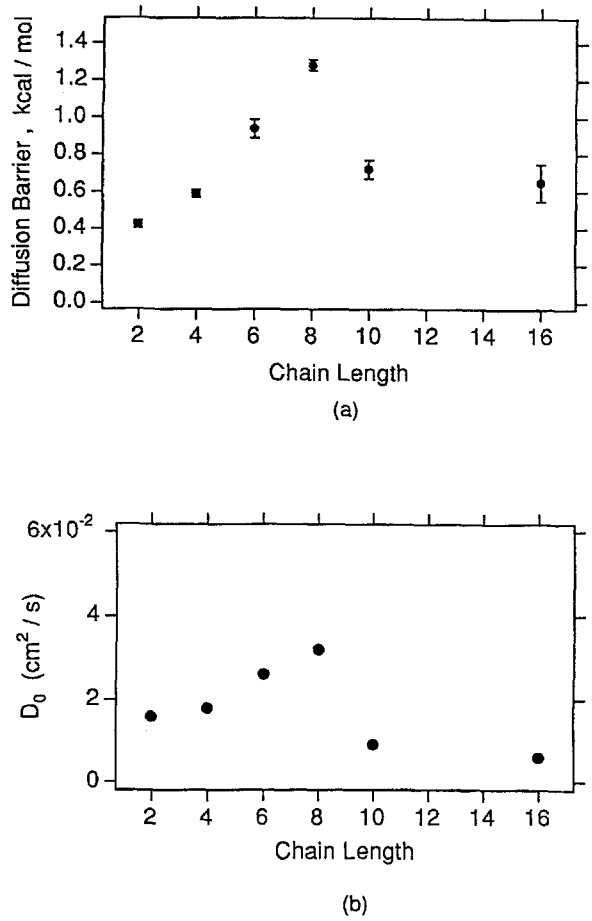

Figure 4. Surface diffusion energy barrier (a) and preexponential factor (b) as a function of chain length. The error bars in (a) are one standard deviation.

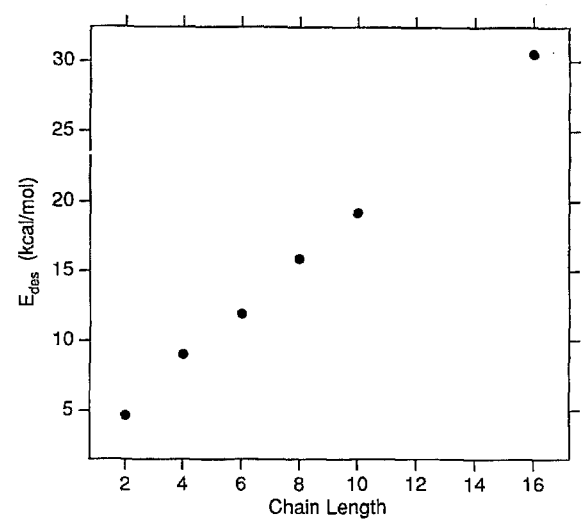

Figure 5. Desorption activation energy as a function of chain length.

It should be noted that the potential energy did not vary significantly with temperature over the range probed in our study. The values of the desorption activation energy E_{des} are depicted as a function of chain length in Fig. 5.

As shown in Fig. 4(a) the surface diffusion activation energies of ethane, *n*-butane, *n*-hexane, and *n*-octane increase almost linearly with the carbon chain length. However, the diffusion barriers of decane and hexadecane fall below the barrier of hexane. Unlike the trend shown for E_d, the values of E_{des} increase linearly with chain length for all *n*-alkanes, as shown in Fig. 5. The linear dependence of E_{des} on carbon chain length stems from the similarity of adsorption conformations for the *n*-alkane series (Huang et al., 1994a). At the minimum-energy binding conformation, the molecules lie "flat", in the all-*trans* conformation, with their long axes parallel to the surface plane and each united atom residing close to a three-fold site on the surface. Bond-angle bending is negligible. At low temperatures, adsorption of the molecules is mostly localized to these conformations. We began to observe an increasing fraction of conformational isomers, with some of the torsion angles in the *gauche* state, for temperatures at and above 200 K. However, even at these temperatures, the molecules remain in the all-*trans* state for greater than 75% of the time.

The observed adsorption conformations are consistent with findings from low-energy electron diffraction (Firment and Somorjai, 1977) and infrared spectroscopy (Chesters et al., 1989) studies of *n*-alkanes on Pt(111). A similar trend in binding energy has been found for *n*-alkanes adsorbed on Cu(001) (Sexton and Hughes, 1984). Our findings are also consistent with the LITD experimental results of Brand et al. (1990), who studied the diffusion of a series of *n*-alkanes, ranging in size from propane to *n*-hexane, on Ru(001). In their study, Brand et al. (1990) found that both E_d and E_{des} increased linearly with increasing chain length and suggested that the linear trends implied that the molecules have similar binding configurations and similar diffusion mechanisms. We would like to relate the trend in the measured diffusion barriers to characteristic diffusion mechanisms of the molecules.

Using the Elastic-Band method, as discussed above, we determined minimum-energy paths for motion of ethane through *n*-decane between neighboring binding sites. For each of these molecules, the center of mass

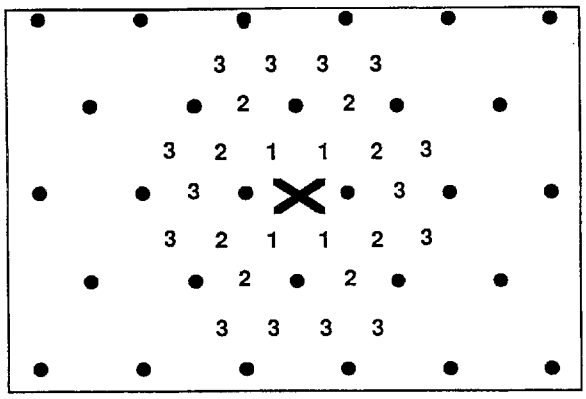

Figure 6. First (1), second (2) and third (3) neighbors of a molecule with center of mass at a bridge site (X) on the Pt(111) surface. Neighbors are defined in terms of the number of single-site hops required to reach them. Filled circles represent locations of Pt surface atoms.

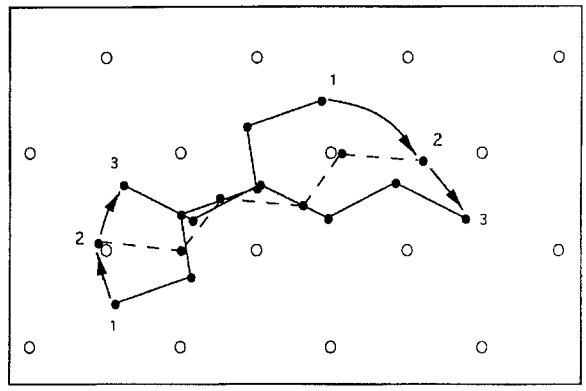

Figure 7. Top-down view of sequences of molecular conformations along the minimum-energy path for motion between neighboring binding sites of *n*-hexane. Conformations 1 and 3 are the conformations of the molecule in the initial and final binding sites, respectively. Conformation 2 is the transition-state conformation. Arrows indicate the approximate pathway for the motion. Open circles represent locations of Pt surface atoms.

at the global-minimum-energy binding site is located between two neighboring Pt atoms (i.e., at the bridge site) on Pt (111), as shown in Fig. 6. The bridge site has four nearest-neighbor sites, 8 second neighbors and 14 third neighbors. Here, we define neighbors in terms of the number of single-site hops that are required to reach them. Not all of the neighbors of a given type are the same distance from the bridge site. Moreover, different diffusion mechanisms may be necessary to reach neighbors that are the same distance from the bridge site. In our studies, we considered hops between global minima at these different distances. In similar studies (Sanders and DePristo, 1992; Liu et al., 1992), conducted for atomic surface diffusion, only nearest-neighbor hops were considered, since atomic size and symmetry considerations indicated, in these cases, that hops to more distant neighbors were comprised of several nearest-neighbor hops. However, it is not obvious, especially as the size of the molecule increases relative to the nearest-neighbor distance, that the minimum-energy path for hopping between nearest-neighbor sites has a lower energy barrier than that for hopping between more distant neighbors. In addition to considering hops of molecules between global minima, we have also considered hops involving local minima, which begin to appear with increasing chain length. A full discussion of these results will be presented elsewhere (Chen and Fichthorn, 1995). Here, we show some illustrative examples.

Figure 7 shows molecular sequences along the minimum-energy path for hexane to diffuse to a nearest-neighbor binding site on the Pt(111) surface. It is evident that the nearest-neighbor hopping mechanism involves coupled translation and rotation of the molecule in the surface plane. All of the molecules that we studied in the static calculations (ethane-decane) exhibit similar mechanisms for nearest-neighbor hopping (Huang et al., 1994a). In the MD simulations, we observed that all of the molecules exhibit this type of mechanism, to varying extents. In the rigid-rod rotation mechanism for nearest-neighbor hopping, an increasing number of united atoms must pass close to surface atoms as the molecular chain length increases, leading to an increase in the diffusion barrier with increasing chain length. As can be seen in Fig. 8, the diffusion barriers for nearest-neighbor hopping of ethane through hexane increase linearly with increasing molecular size. However, the nearest-neighbor hopping barrier for octane and decane show a departure, with a decrease in slope, from the trend exhibited by the shorter molecules.

A comparison of the "dynamical" diffusion barriers (cf. Fig. 4(a)), obtained from MD simulation, to the "static" barriers for nearest-neighbor hopping (Fig. 8) shows good agreement for butane, hexane, and octane. The deviations seen for ethane arise because of the very small static diffusion barrier for that molecule, as discussed elsewhere (Huang et al., 1994a, b; Raut and Fichthorn, 1995). Briefly, in the hopping model, the diffusion coefficient D (cf. Eq. (6)) is given by

$$D = \frac{n\lambda^2\nu_0}{4}\exp\left(-\frac{E_d}{RT}\right). \qquad (7)$$

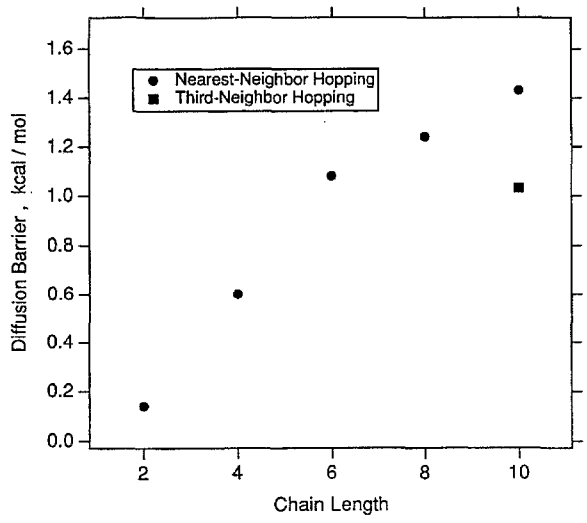

Figure 8. Diffusion barriers calculated for nearest-neighbor hopping as a function of chain length. The barrier for third-neighbor hopping of decane has been calculated for the pathway shown in Fig. 10.

where n is the number of hopping directions, ν_0 is the frequency factor, and λ is the hopping length. In analysis of data, it is assumed that the hopping length is constant and that the primary temperature dependence of D is in the exponential, with a mild temperature dependence of ν_0. However, in the simulations, the hopping length is not independent of temperature and ethane shows an increasing fraction of long jumps with increasing temperature. Moreover, adsorption becomes increasingly delocalized with increasing temperature (Raut and Fichthorn, 1995). Both of these factors can significantly influence the value of the diffusion coefficient at a given temperature, as well as the value of E_d that is obtained from an Arrhenius plot.

The departure of the diffusion barriers of decane and hexadecane from the linear trend seen for the shorter molecules (cf. Fig. 4(a)) and from the linear trend predicted by TST for nearest-neighbor hopping (cf. Fig. 8) could have several origins, which are currently under investigation. Here we discuss some preliminary findings. One contribution to lower barriers for increased chain length is molecule-surface mismatch (Huang et al., 1994a). In the optimal location, each united atom would reside directly above a threefold hollow site on the Pt(111) surface. However, mismatch between the alkane and the Pt(111) geometry does not allow this and some of the united atoms have to reside closely to Pt surface atoms, from which they are repelled. Due to mismatch, which becomes more pronounced with increasing chain length, the molecule-surface potential becomes less corrugated and the value of the diffusion barrier is reduced. This effect contributes to the less-than-linear increase in the static diffusion barriers for nearest-neighbor hopping of octane and decane compared to the trend for the shorter molecules (cf. Fig. 8). However, mismatch, by itself, cannot completely explain the trend in the dynamical barriers for decane and hexadecane, since it does not lead to a substantial decrease in the diffusion energy.

The decrease in the diffusion barriers for decane and hexadecane might be explained by a change in the characteristic diffusion mechanisms for these molecules. Looking to computer animation for guidance, we observed several mechanisms for the longer molecules. Some of the motion appears to be rigid rod-like, although, unlike the shorter molecules, we observed hops, involving unique mechanisms, to second- and third-neighbor sites. Figure 9 shows a typical center-of-mass trajectory for decane at 75 K. Two types of hops can be seen in Fig. 9, in addition to several long flights. In the most commonly observed mechanism, decane hops to a third-neighbor site via two consecutive small-angle rotations over the top of a Pt surface atom. A three-step sequence of this mechanism is

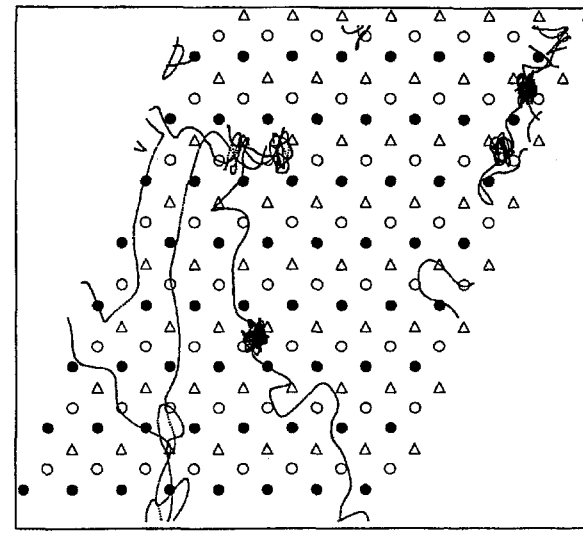

Figure 9. The trajectory of the center of mass of n-decane at 75 K. The filled circles represent first-layer Pt atoms, the open circles represent second-layer Pt atoms, and the triangles represent third-layer Pt atoms.

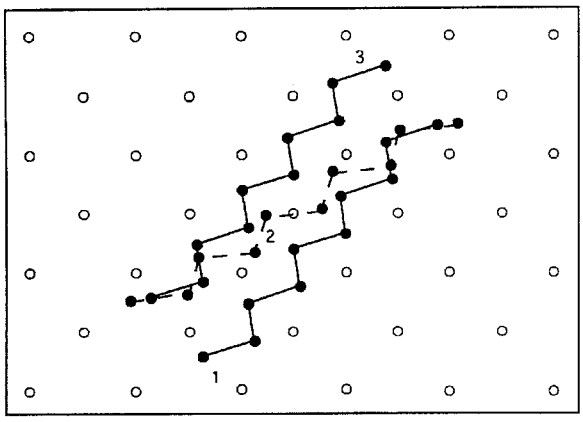

Figure 10. Top-down view of the three-step sequence of third-neighbor hopping mechanism for decane. Conformations 1 and 3 are the conformations of the molecule in the initial and final binding sites, respectively. Conformation 2 is the transition-state conformation. Open circles represent locations of Pt surface atoms.

shown in Fig. 10. Decane has a shallow local minimum in energy when the center of mass is located above a top site, with the conformation shown in Fig. 10, so that the third-neighbor hopping mechanism is actually a two-hop sequence. However, due to the small configurational volume of the local minimum, it was often bypassed. Here, we consider this sequence as a single hop. The energy barrier for this type of motion is depicted in Fig. 8. It can be seen that the energy barrier for this mechanism is lower than the energy barrier for nearest-neighbor hopping of hexane, consistent with the trends in the simulations (cf. Fig. 4(a)). However, the theoretical diffusion energy is still substantially larger than that obtained from the simulations.

It is possible that the motion of the longer molecules involves pathways that we have not yet elucidated. One possibility, that can be observed in the simulations, is motion that is mediated by or that involves significant bond-angle bending. Both decane and hexadecane exhibit more bond angle bending than the shorter alkanes. (It should be noted, however, that the extent to which the C—C—C bonds are bent is still not large.) Increased bond-angle bending relieves some of the molecule-surface mismatch and it may also facilitate motion. Although the mechanisms, that we have investigated up until now, do not involve bond-angle bending as a primary degree of freedom, our search has been limited to motion between global minima and the local minima that could be mapped onto the surface unit cell. It is likely that other local minima exist and it is possible that they could be involved in diffusion mechanisms mediated by bond-angle bending. It is interesting to note that the diffusion barrier of hexadecane is only slightly less than and within the error of that of decane (cf. Fig. 4(a)). There is also evidence, from preliminary simulations, that the diffusion barrier for icosane is about the same as that of hexadecane. If the characteristic diffusion mechanisms of these molecules are segmental (as opposed to the rigid-rod motion that we see for the shorter molecules) and mediated by internal motion, we would anticipate the diffusion barrier to be independent of chain length (Brand et al., 1990). Further investigation should confirm whether or not this is the case.

Finally, it is worth noting that, despite the very good agreement between the static and the dynamical diffusion barriers for some of the molecules, the motion of the n-alkane series does not strongly adhere to the assumptions of the hopping model. Although some hopping can be seen for all of the molecules at low temperatures (see e.g., Fig. 9), long flights occur at all temperatures. At the highest temperatures, adsorption is virtually delocalized for all of the molecules probed. At these temperatures the proportion of the time that the trajectories spend on intersite motion is comparable to the amount of time spent localized at a binding site and the assumptions of the hopping model are no longer valid. Despite this discrepancy, all of the Arrhenius plots are linear and the activation energies for n-butane through n-octane can be obtained by considering only nearest-neighbor hops. One symptom of the discrepancy between the hopping model and the simulations shows up in the preexponential factors, obtained from the simulations, as shown in Fig. 4(b). These appear to be too large (Huang et al., 1994a), a finding that is consistent with other simulation studies (Dobbs and Doren, 1992). If improvement is to be made between theory and simulation (and, most likely, experiment (Brand et al., 1990)), a kinetic theory should be developed that includes long, nonlocalized flights, in addition to hopping motion. A model of this type would provide a more realistic description of the motion.

Conclusions

The surface of n-alkanes, ranging from ethane to hexadecane, physically adsorbed on Pt(111) has been simulated using MD over a wide temperature range. Investigations of the diffusion mechanisms and diffusion-energy barriers have been conducted within the framework of transition-state theory. Our

observations of the adsorption conformations corroborate with findings from low-energy electron diffraction (Firment and Somorjai, 1977) and infrared spectroscopy (Chesters et al., 1989) studies of n-alkanes on Pt(111). The desorption energy increases linearly with chain length, as seen experimentally (Brand et al., 1990). The diffusion activation energies of ethane through n-octane follow the linear scaling trends seen in related experimental studies (Brand et al., 1990). Through both animation of the molecular trajectories and static determination of the minimum-energy path for nearest-neighbor hopping, we find that the shorter molecules (ethane through octane) all have similar diffusion mechanisms, involving coupled translation and rigid-rod-like rotation in the surface plane. The static diffusion-energy barriers, arising from the minimum-energy path for hops between nearest-neighbor binding sites, agree well with those obtained from the tracer-diffusion coefficients for butane, hexane, and octane. We find that the diffusion barrier for ethane does not agree well with theoretical estimates, a discrepancy we attribute to the smallness of the static diffusion barrier for this molecule (Huang et al., 1994; Raut and Fichthorn, 1995). The diffusion of decane and hexadecane does not adhere to the trends for the shorter molecules and a decrease can be observed in the diffusion energies for these molecules. The diffusion of the longer molecules involves hops, with unique mechanisms, to second and third neighbor sites. Our analysis has indicated, for decane, that the diffusion-energy barrier for third-neighbor hopping, across a top site, is lower than that for nearest neighbor hopping and is lower than the static diffusion barrier for nearest-neighbor hopping of hexane. Computer animation has also revealed that the motion of the longer molecules involves more bond-angle bending than that of the shorter molecules. Even though there is agreement between theoretical and simulated diffusion energy barriers for many of the molecules, the motion observed in the MD simulations does not agree with the assumptions of the hopping model. A model that can incorporate the influence of long flights would provide a more realistic description of the motion.

Nomenclature

d_{CC}	equilibrium carbon-carbon bond length in the fluid phase	m
D	diffusion coefficient	cm^2/s
D_0	preexponential factor for diffusion	cm^2/s
E_d	activation energy for diffusion	kJ/mol or kcal/mol
E_{des}	binding energy	kJ/mol or kcal/mol
k	spring constant	J/m^2
$\langle l^2 \rangle$	mean-square displacement	m^2
m_i	mass of particle i	kg
n	number of hopping directions	
$\boldsymbol{p}_i$	momentum of particle i	kg-m/s
P	number of images	
$\boldsymbol{r}_i$	position of particle i	m
R	Ideal Gas constant	J/mol-K
$\boldsymbol{R}_i$	configuration of n-alkane i	m
t	time	s
T	temperature	K
U	potential energy	J
U^s	spring energy	J
ε_{ms}	Lennard-Jones energy parameter for interaction between united atoms and surface atoms	J/mol
λ	hopping length	m
λ_k	Lagrange multiplier for kth carbon-carbon bond	Kg/g^2
ν_0	frequency factor	s^{-1}
σ_k	constraint condition on carbon-carbon bond length	m^2
σ_{ms}	Lennard-Jones length parameter for interaction between united atoms and surface atoms	m
σ_s	Lennard-Jones length parameter for interaction between surface atoms	m
ζ	friction coefficient	s^{-1}

Acknowledgments

This work was funded by the National Science Foundation under grant CTS-9058013. The computer workstations were provided by NSF equipment grant CTS-9112468. Acknowledgment is made to the donors of the Petroleum Research Fund, administered by the ACS, for partial support of this research. K. A. F. thanks Mr. Jee-Ching Wang and Mr. Yin Chen, for supplying some of the figures.

References

Allen, M.P. and D.J. Tildesley, *Computer Simulation of Liquids*, Clarendon Press, Oxford, 1987.

Allen, R.E., G.P. Alldredge, and F.W. deWette, "Studies of vibrational surface modes, II monoatomic fcc crystals," *Phys. Rev.*, **B4**, 1661 (1971).

Arena, M.V., A.A. Deckert, J.L. Brand, and S.M. George, "Surface diffusion and desorption of pentane isomers on Ru(001)," *J. Phys. Chem.*, **94**, 6792 (1990).

Brand, J.L., M.V. Arena, A.A. Deckert, and S.M. George, "Surface diffusion of *n*-alkanes on Ru(001)," *J. Chem. Phys.*, **92**, 5136 (1990).

Brown, D. and J.H.R. Clarke, "A comparison of constant energy, constant temperature, and constant pressure ensembles in molecular dynamics simulations of atomic liquids," *Mol. Phys.*, **51**, 1243 (1984).

Catlow, C.R.A., S.C. Parker, and M.P. Allen, *Computer Modelling of Fluids Polymers and Solids*, NATO ASI Series C, Kluwer Academic Publishers, 1990.

Chen, Y. and K.A. Fichthorn, "Diffusion mechanisms of *n*-alkanes adsorbed on Pt(111)," (to be published).

Chesters, M.A., P. Gardner, and E.M. McCash, "The reflection-absorption infrared spectra of *n*-alkanes adsorbed on Pt(111)," *Surf. Sci.*, **209**, 89 (1989).

Cohen, J.M. and A.F. Voter, "Self-diffusion on the Lennard-Jones fcc(111) surface: Effects of temperature on dynamical corrections," *J. Chem. Phys.*, **91**, 5082 (1989).

Dobbs, K.D. and D. Doren, "Dynamics of molecular surface diffusion: Origins and consequences of long jumps," *J. Chem. Phys.*, **97**, 3722 (1992).

Evans, D.J., "Computer experiment for nonlinear thermodynamics of Couette flow," *J. Chem. Phys.*, **78**, 3297 (1983).

Fichthorn, K.A., P. Balan, and Y. Chen, "Simulation and analysis of the motion of *n*-butane on Pt(111)," *Surf. Sci.*, **317**, 37 (1994).

Firment, L.E. and G.E. Somorjai,., "Surface structures of normal paraffins and cyclohexane monolayers and thin crystals grown on the (111) crystal face of platinum: A low-energy electron diffraction study," *J. Chem. Phys.*, **66**, 2901 (1977).

Fixman, M., *Proc. Nat. Acad. Sci.*, **71**, 3050 (1974).

Ganz, E.S., S.K. Thesis, I. Hwang, and J. Golvochenko, "Direct measurement of diffusion by hot tunneling microscopy: Activation energy, anisotropy, and long jumps," *Phys. Rev. Lett.*, **68**, 1567 (1992).

Hallmark, V.M., S. Chiang, K.-P. Meinhardt, and K. Hafner, "Observation and calculation of internal structure in scanning tunneling microscopy images of related molecules," *Phys. Rev. Lett.*, **70**, 3740 (1993).

Huang., D., Y. Chen, and K.A. Fichthorn, "The diffusion dynamics of short *n*-alkanes on smooth metal surfaces," *J. Chem. Phys.*, **101**, 11021 (1994).

Huang, D., P. Balan, Y. Chen, and K.A. Fichthron, "Molecular-dynamics simulation of the diffusion of *n*-alkanes on Pt(111)," *Molecular Simulation*, **13**, 285 (1994).

Hoover, W.G., A. J. C. Ladd, and B. Moran,, "High strain rate plastic flow studied via nonequilibrium molecular dynamics," *Phys. Rev. Lett.*, **48**, 1818 (1982).

Ionova, I.V. and E.A. Carter, , "Ridge method for finding saddle points on potential energy surfaces," *J. Chem. Phys.*, **98**, 6377 (1993).

Liu, C.L., J.M. Cohen, J.B. Adams, and A.F. Voter, "EAM study of surface self-diffusion of single atoms on fcc metals Ni, Cu, Al, Ag, Au, Pd, and Pt," *Surf. Sci.*, **253**, 334 (1991).

Mills, G. and H. Jónsson, "A method for finding optimal transition paths: Application to diffusion on metal surfaces," submitted to *J. Chem. Phys.*

Mills, G. and H. Jónsson, "Quantum thermal effects in H2 dissociative adsorption: Evaluation of free energy barriers in multidimensional systems," *Phys. Rev. Lett.*, **72**, 1124 (1994)

Nosé, S., "Constant temperature molecular dynamics methods," *Prog. Theor. Phys., Supplement No. 103*, **1** (1991).

Raut, J.S. and K.A. Fichthorn, "Tracer-diffusion coefficients for both localized and non-localized adsorption: Theory and molecular-dynamics simulation," *J. Chem. Phys.*, **103**, 8694 (1995).

Reutt-Robey, J.E., D.J. Doren, Y.J. Chabal, and S.B. Christman, "Microscopic CO diffusion on a Pt(111) surface by time-resolved infrared spectroscopy," *Phys. Rev. Lett.*, **61**, 2778 (1988).

Ryckaert, J.P. and A. Bellemans,"Molecular dynamics of liquid alkanes," *Faraday. Discuss. Chem. Soc.*, **66**, 95 (1978).

Ryckaert, J.P., G. Ciccotti, and H.J.C. Berendsen, "Numerical integration of the Cartesian equations of motion of a system with constraints: molecular dynamics of *n*-alkanes," *J. Comp. Phys.*, **23**, 327 (1977).

Salmeron, M. and G.A. Somorjai, "Adsorption and bonding of butane and pentane on the Pt(111) crystal surface: Effect of oxygen treatments and deuterium preadsorption," *J. Phys. Chem.*, **85**, 3840 (1981).

Sanders, D.E. and A.E. DePristo, "Predicted diffusion rates on fcc(001) metal surfaces for adsorbate/substrate combinations of Ni Cu, Rh, Pd, Ag, Pt, Au," *Surf. Sci.*, **260**, 116 (1992).

Sevick, E.M., A.T. Bell, and D.B. Theodorou, "Chain of states method for investigating infrequent event processes occurring in multistate, multidimensional systems," *J. Chem. Phys.*, **98**, 3196 (1993).

Sexton, B.A. and A.E. Hughes, "A comparison of weak molecular adsorption of organic molecules on clean copper and platinum surfaces," *Surf. Sci.*, **140**, 227 (1984).

Stranick, S.J., M.M. Kamna, and P.S. Weiss, "Atomic-scale dynamics of a two-dimensional gas-solid interface," *Science*, **266**, 99 (1994).

van der Ploeg, P. and H.J.C. Berendsen, "Molecular dynamics of a bilayer membrane," *Mol. Phys.*, **85**, 1613 (1986).

Wang, J.-C. and K.A. Fichthorn, "Diffusion mechanisms of physically adsorbed dimers on fcc(100) surfaces," to appear in *Langmuir*.

Wang, R. and K.A. Fichthorn, "Diffusion mechanisms of dimers adsorbed on periodic substrates," *Phys. Rev.*, **B48**, 18288 (1993).